The Astrophysical Journal Letters, 922:L12 (5pp), 2021 November 20 https://doi.org/10.3847/2041-8213/ac3663
© 2021. The Author(s). Published by the American Astronomical Society.
OPEN ACCESS

Prediction of Sunspot and Plage Coverage for Solar Cycle 25

Valentina Penza[1], Francesco Berrilli[1], Luca Bertello[2], Matteo Cantoresi[1], and Serena Criscuoli[2]
[1] Dipartimento di Fisica, Università di Roma Tor Vergata, Via della Ricerca Scientifica 1, I-00133 Roma, Italy
[2] National Solar Observatory, 3665 Discovery Drive, Boulder, CO 80303, USA; scriscuo@nso.edu
Received 2021 October 4; revised 2021 October 26; accepted 2021 November 3; published 2021 November 18

Abstract

Solar variability occurs over a broad range of spatial and temporal scales, from the Sun's brightening over its lifetime to the fluctuations commonly associated with magnetic activity over minutes to years. The latter activity includes most prominently the 11 yr sunspot solar cycle and its modulations. Space weather events, in the form of solar flares, solar energetic particles, coronal mass ejections, and geomagnetic storms, have long been known to approximately follow the solar cycle occurring more frequently at solar maximum than solar minimum. These events can significantly impact our advanced technologies and critical infrastructures, making the prediction for the strength of future solar cycles particularly important. Several methods have been proposed to predict the strength of the next solar cycle, cycle 25, with results that are generally not always consistent. Most of these methods are based on the international sunspot number time series, or other indicators of solar activity. We present here a new approach that uses more than 100 yr of measured fractional areas of the visible solar disk covered by sunspots and plages and an empirical relationship for each of these two indices of solar activity in even–odd cycles. We anticipate that cycle 25 will peak in 2024 and will last for about 12 yr, slightly longer than cycle 24. We also found that, in terms of sunspot and plage areas coverage, the amplitude of cycle 25 will be substantially similar or slightly higher than cycle 24.

Unified Astronomy Thesaurus concepts: Solar activity (1475); Solar cycle (1487); Solar faculae (1494); Sunspot cycle (1650)

1. Introduction

The variability of the Sun's magnetic activity is the main driver of changes in the near-Earth space environment, the heliosphere, and the interplanetary medium. This variability is characterized by a large number of phenomena that act over a wide range of temporal scales, from minutes to centuries. A particularly important class of short-lived phenomena, up to a few days, includes events such as solar flares and coronal mass ejections that are responsible for the space weather. These events have a significant impact on the functionality of satellites, communication networks, electric power grid, and technological infrastructures (e.g., Schwenn 2006; Plainaki et al. 2020). Instead, solar activity over longer timescales modifies the so-called space climate (Versteegh 2005) that contributes to determining the conditions of Earth's upper and lower atmosphere and Earth's climate (e.g., Bordi et al. 2015; Matthes et al. 2017; Bigazzi et al. 2020; Lockwood & Ball 2020) and the cosmic-ray fluxes in the interplanetary space and at Earth (e.g., Usoskin et al. 2002; Berrilli et al. 2014; Fiandrini et al. 2021). Similarly, stellar irradiance and its variations affect exoplanets' atmospheres and their habitability (e.g., Meadows & Barnes 2018; Galuzzo et al. 2021). The most evident modulation of the large-scale solar magnetic field is its 11 yr cycle, during which the Sun increases and weakens its magnetic activity, associated with a reversal of the dominant polarities in the polar regions. This cycle is accompanied by variations in phase of the appearance of magnetic structures on the solar surface, such as sunspots and plages. The dark sunspots produce a luminosity defect, while the bright plages overcompensate with an excess (e.g., Foukal & Lean 1988). The final result is that the total solar irradiance varies by about 0.1%, in phase with the magnetic activity (e.g., Wilson 1978; Hudson 1988; Kopp et al. 2016). The strength of the different cycles is not constant, and can vary quite significantly as indicated by the presence of grand minimum periods (e.g., Vecchio et al. 2017) such as the Maunder minimum during the years of 1645–1715 (e.g., Hathaway 2015).

The capability of predicting the behavior of the solar activity has become of paramount relevance, given its enormous impact on human activities on Earth and in space. Providing a detailed description of the literature regarding the prediction of the next 25th solar cycle (hereafter SC25) is beyond the scope of this Letter. We therefore refer to the review of solar cycle prediction methods, with particular focus on forecasts for SC25, given in Petrovay (2020). The various forecasts differ in the adopted methodology (e.g., surface flux transport models, identification of particular "termination" events, Shannon entropy estimates, machine learning regression methods, etc.) and in the physical observable on which the prediction is based. In particular, the methods typically fall into three categories: precursor, model-based, and extrapolation methods. For the prediction of SC25 different studies have been published that use the sunspot number (e.g., McIntosh et al. 2020; Singh et al. 2021), the geomagnetic activity indices (e.g., Singh et al. 2021), the flare number (e.g., Janssens 2021), and the solar magnetic flux or dipole momentum (e.g., Cameron et al. 2016; Bhowmik & Nandy 2018; Upton & Hathaway 2018; Labonville et al. 2019).

The aim of this work is to estimate the coverage of sunspot and plage areas during the next SC25. We use an appropriate functional form for solar cycles derived from the correlation between cycles for the period 1874–2019. This approach has two important aspects: first, it is based on the observed characteristics of the cycles and does not use sophisticated

Original content from this work may be used under the terms of the Creative Commons Attribution 4.0 licence. Any further distribution of this work must maintain attribution to the author(s) and the title of the work, journal citation and DOI.

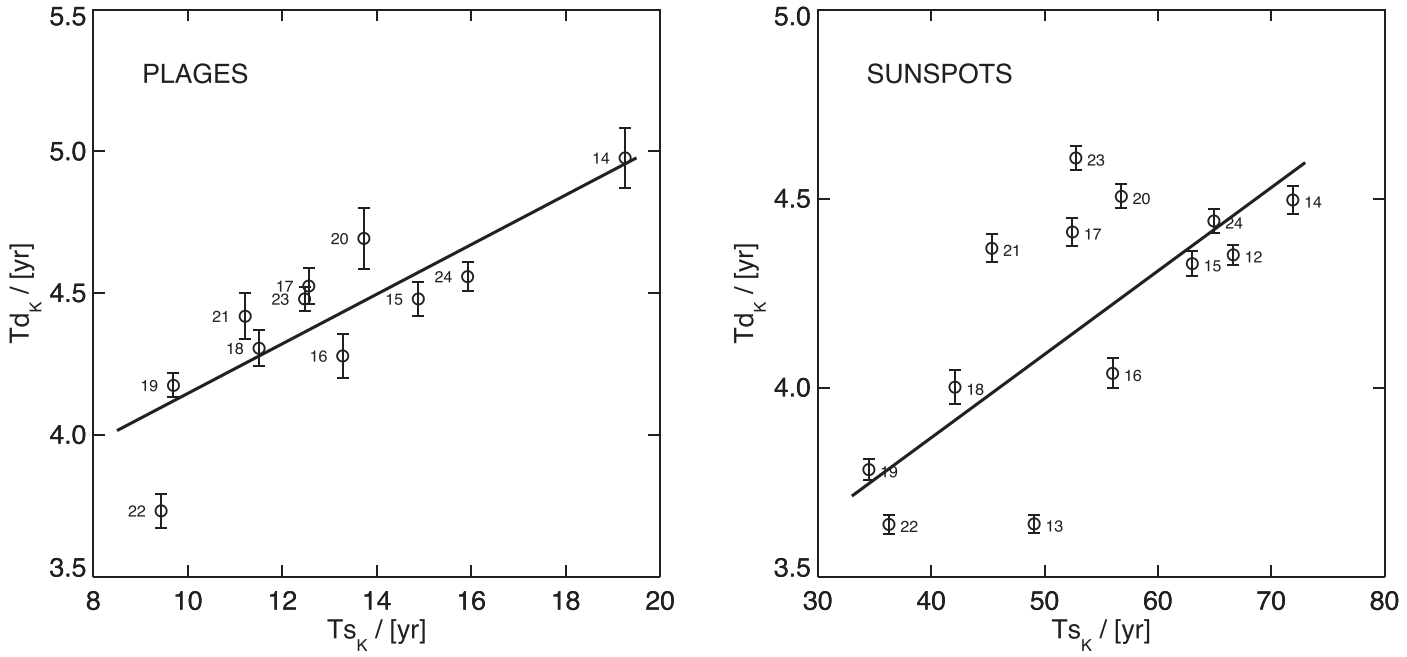

Figure 1. Solar cycle-to-cycle relationship between the parameters Td_k and Ts_k for plage (left) and sunspot (right) areas. Two additional solar cycle numbers, 12 and 13, have been included in the analysis of sunspot areas. The open circles with 1σ error bars show the data averaged over individual cycles. The regression lines (continuous lines) are given by Equation (2).

physical models that unfortunately suffer from the difficulties connected to the complex physical processes involved and to the inherent dynamical complexity of the solar cycle (e.g., Bushby & Mason 2004; Consolini et al. 2009; Charbonneau 2020); second, the coverage in the area of sunspots and plages can be used as proxies to predict other activity indices important for space climate, including spectral and total solar irradiance variability (e.g., Foukal & Lean 1988; Berrilli et al. 2020; Petrie et al. 2021).

2. Active Region Parameterization

We characterize the shape of each solar cycle through a unique functional form. Among those proposed in the literature (e.g., Baranovski et al. 2008; Hathaway et al. 1994), we choose the following parametric fit suggested in Volobuev (2009):

$$x_k(t) = \left(\frac{t - T0_k}{Ts_k}\right)^2 e^{-\left(\frac{t-T0_k}{Td_k}\right)^2} \quad \text{for} \quad T0_k < t < T0_k + \tau_k, \tag{1}$$

where $T0_k$ is the initial time of cycle k (published in Hathaway et al. 1994; Hathaway 2015), while Ts_k and Td_k are two free parameters. As discussed in Volobuev (2009), there is a strong linear correlation between these two parameters, which reduces the fit to a single parameter (Ts_k). This is not surprising, because the Ts_k parameter is related to the time of the rising phase, while the Td_k value determines the cycle amplitude. The relation between these two quantities is known and reported in the literature: cycles with large amplitude (smaller Ts_k) present a shorter time of rising to maximum (shorter Td_k). This is known as the Waldmeier effect (e.g., Hathaway et al. 1994; Hazra et al. 2015).

We adopt Equation (1) to fit, cycle by cycle, the plage and sunspot coverage data. For this purpose we used two data sets (composites) available from the Max Plank Institute website.[3] The first composite consists of plage area derived from Ca II K spectroheliogram observations covering the period 1892–2019 (Chatzistergos et al. 2019). The second composite includes measurements of daily total sunspot area for the period 1874–2019, calculated after cross-calibration of measurements by different observers (Mandal et al. 2020). The relation between the Ts_k and Td_k for plage and sunspot areas is shown in Figure 1. A linear fit to these data produces

$$\begin{aligned} Td_k^{\text{plage}} &= (0.09 \pm 0.01)\, Ts_k^{\text{plage}} + (3.27 \pm 0.10)\ yr \\ Td_k^{\text{spot}} &= (0.022 \pm 0.001)\, Ts_k^{\text{spot}} + (2.98 \pm 0.04)\ yr. \end{aligned} \tag{2}$$

The Pearson correlation coefficients are r = 0.81 and r = 0.72 for plage and spot fit, respectively. A t-test was performed to determine the statistical significance of the computed correlation coefficients. We found there is a nonzero correlation between Ts_k and Td_k, at a confidence level greater than 99% for the plages and greater than 95% for the sunspots.

By inserting these relationships in Equation (1), we obtain a one-parameter functional form for the shape of the cycles. We repeat the fits, cycle by cycle, and we obtain two data sets of Ts_k values.

The active region coverages ($A(t)_{\text{plage}}$ and $A(t)_{\text{spot}}$) for the entire analyzed period are thus reproduced as

$$A(t) = \sum_k x_k(t), \tag{3}$$

where the cycle number k goes from the 14th (begin data = 1902 January) to the 23rd (begin data = 1996 August) for plage data and from the 12th (begin data = 1878 December) for sunspot data. The parametric reconstructions for plage and

[3] http://www2.mps.mpg.de/projects/sun-climate/data.html

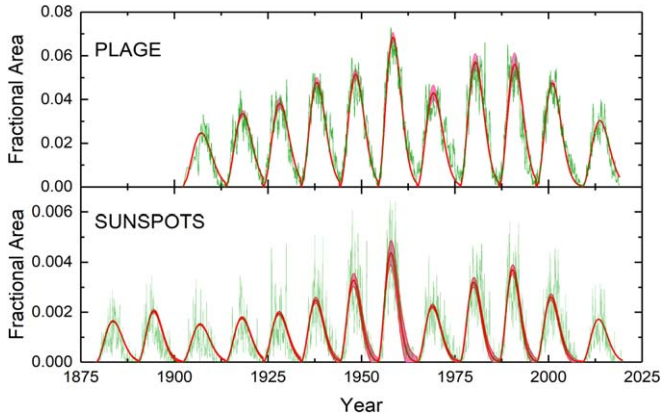

Figure 2. Top panel: reconstructed plage area (red solid line) with a confidence range (light red pattern) and observed plage composite (green solid line) by Chatzistergos et al. (2019). Bottom panel: reconstructed sunspot area (red solid line) with a confidence range (light red pattern) and observed sunspot area composite (green solid line) from Mandal et al. (2020). It should be noted that our method has been developed in order to provide an estimate of the coverage of plage and sunspots on an annual scale and therefore cannot reproduce shorter timescale variability (e.g., months). This explains the difference between the observed plage and sunspot coverages (green solid lines) and the reconstructed ones (red solid line). The ability to capture long-term behavior by the functional form is also evident.

sunspot area are shown in Figure 2. A confidence region is estimated by taking into account the errors on the fit parameters.

3. Relation between Even and Odd Cycles

Through the fits of the observed active region coverages, we have obtained the single parameter characterizing the last 11 cycles for the plages and the last 13 cycles for the sunspots.

We couple these values in pairs, i.e., as even–odd cycles, taking into account that the complete magnetic cycle of the Sun is composed of two consecutive cycles. By plotting the even–odd parameters, one versus the other, we obtain the correlations shown in Figure 3, whose fits are as follows:

$$Ts_o^{\rm plage} = (0.74 \pm 0.08)\, Ts_e^{\rm plage} + (1.5 \pm 1.1)\ yr$$
$$Ts_o^{\rm spot} = (0.69 \pm 0.05)\, Ts_e^{\rm spot} + (11 \pm 3)\ yr, \quad (4)$$

where the subscript "e" means "even" and "o" means "odd." The Pearson correlation coefficient is 0.86 for both fits, at a confidence level greater than 90% and 95% for the plages and sunspots, respectively. We highlight the fact that by coupling the parameters in an odd–even manner (e.g., cycle 15 with cycle 16) the correlation is completely lost. This is in agreement with the well-known empirically derived Gnevyshev–Ohl rule (Gnevyshevl & Ohl 1948), which states that the strength of an even cycle is lower than the strength of the subsequent odd cycle.

By inserting the Ts_{24} values derived from sunspot and plage observations and $T0_{25}$ corresponding to 2019 December in Equation (4), we are able to estimate the Ts_{25} values and therefore the shape of the variation of sunspot and plage areas over SC25 using Equation (1). Results are illustrated in Figure 4. The confidence levels shown in the figure are the envelopes of the curves computed by varying the $T_{s_{25}}$ and $T_{d_{25}}$ values within their 1σ confidence level in Equation (1). The plot shows that the maximum of the plage area will occur in 2024 April, with an uncertainty of three months, and that the maximum sunspot area coverage will occur in 2024 January, with an uncertainty of two months. The plots also show that, within the confidence level, the amplitudes of the area coverage of sunspot and plage are similar or slightly higher to those observed during cycle 24.

4. Conclusions

We have presented a prediction of the area coverage of sunspot and plages during solar cycle 25. Our method is based on the empirical correlation between the shapes (amplitude and duration) of even and odd cycles derived from the analysis of

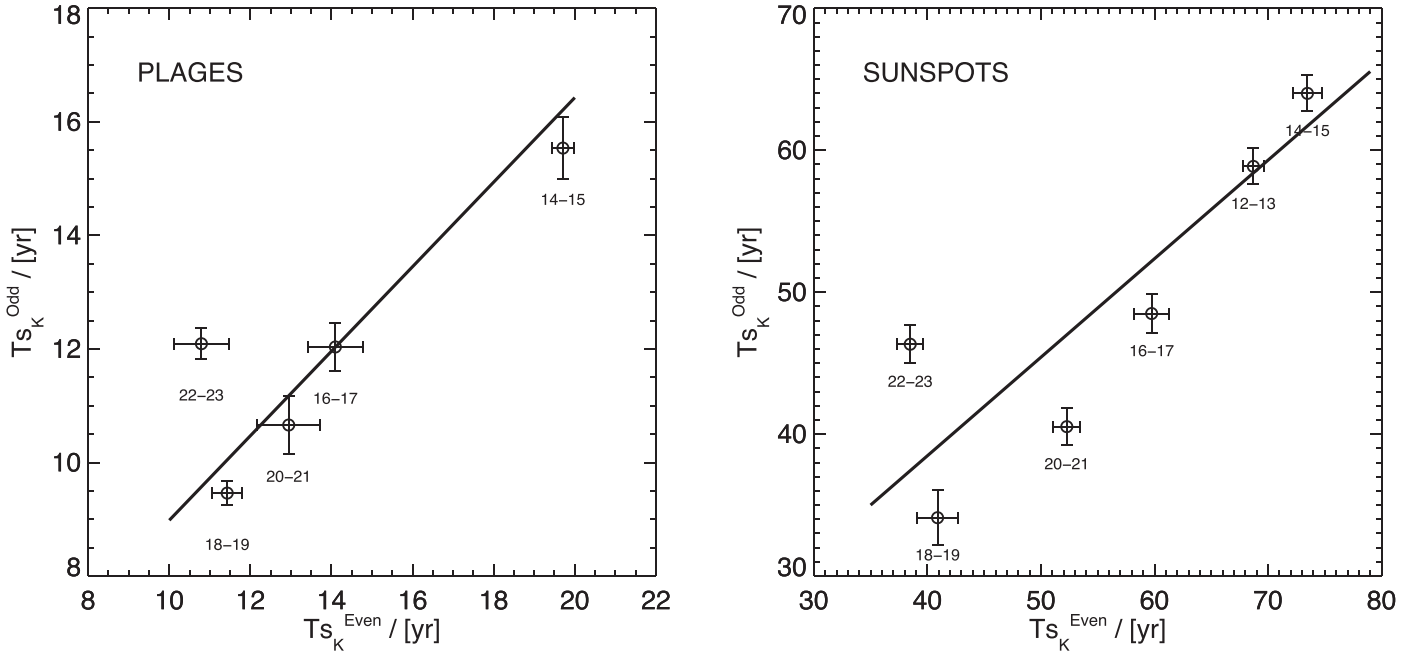

Figure 3. Even–odd cycle relationship between the parameters Ts_k for plage (left) and sunspot (right) areas. The open circles with 1σ error bars in both directions show the cycle-averaged pair of data. The regression lines (continuous lines), given by Equation (4), were computed using the procedure described in Press et al. (1992).

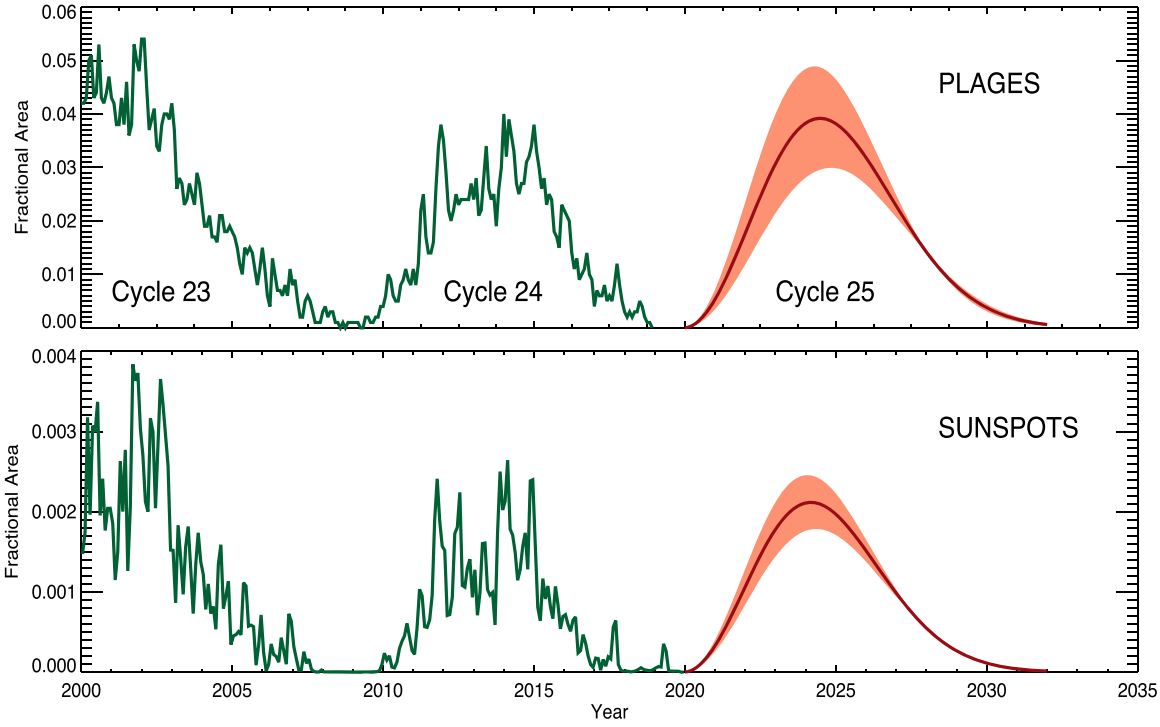

Figure 4. Top panel: observed monthly plage coverage (green curve) during cycles 23–24, and the prediction for cycle 25 (red curve). The shadow red area defines the lower and upper limits for the prediction. Bottom panel: same as the top panel, but for sunspot coverage.

more than 100 yr of observations. Similar relations between properties of subsequent cycles, in particular the even–odd cycle relation, have been empirically derived by using solar sunspot number and other activity proxies in numerous studies (e.g., Mursula et al. 2001; Gupta et al. 2007; Tlatov 2013; Takalo & Mursula 2020; Takalo 2021). Although some authors suggested that the even–odd relation might be the signature of a relic magnetic field (Mursula et al. 2001, and references therein), the physical mechanisms responsible for the even–odd relation are not clear (Hathaway 2015), and it is worth noting that the relation has been questioned by some authors (Zolotova & Ponyavin 2015).

The plage area maximum is predicted for 2024 April, with an uncertainty of about three months, while the sunspot area maximum is predicted for 2024 January, with an uncertainty of about two months. By combining these two results and by assuming a perfect phase between the two quantities, we can hypothesize the maximum intensity level of the SC25 will be in 2024 February–March. By assuming that the sunspot and plage coverage are indicative of the cycle intensity, our prediction is a level of solar activity for the SC25 similar to or slightly higher than that of SC24. This is in agreement with most of the forecasts presented in the literature or using the first available values of the smoothed solar sunspot number (e.g., Bhowmik & Nandy 2018; Petrovay 2020; Carrasco & Vaquero 2021) and with the conclusions of the international NOAA/NASA co-chaired SC25 Prediction Panel.

We want to stress here that our approach is, to our knowledge, the only one that provides a forecast for the coverage of plage and sunspot areas. These quantities are proxies of the solar magnetic activity, can be used to derive other activity indices important for space climate (e.g., Mg II, F10.7, flare indices, etc.) and are fundamental ingredients to estimate both total and spectral irradiance variability.

The authors are grateful to Dr. Lisa Upton for providing insightful comments on an early version of the manuscript. The National Solar Observatory is operated by the Association of Universities for Research in Astronomy, Inc. (AURA), under cooperative agreement with the National Science Foundation. M.C. is supported by the Joint Research PhD Program in "Astronomy, Astrophysics and Space Science" between the universities of Roma Tor Vergata and Roma Sapienza, and INAF.

ORCID iDs

Valentina Penza https://orcid.org/0000-0002-3948-2268
Francesco Berrilli https://orcid.org/0000-0002-2276-3733
Luca Bertello https://orcid.org/0000-0002-1155-7141
Matteo Cantoresi https://orcid.org/0000-0003-4898-2683
Serena Criscuoli https://orcid.org/0000-0002-4525-9038

References

Baranovski, A. L., Clette1, F., & Nollau, V. 2008, AnGeo, 26, 231
Berrilli, F., Casolino, M., Del Moro, D., et al. 2014, JSWSC, 4, A16
Berrilli, F., Criscuoli, S., Penza, V., & Lovric, M. 2020, SoPh, 295, 38
Bhowmik, P., & Nandy, D. 2018, NatCo, 9, 5209
Bigazzi, A., Cauli, C., & Berrilli, F. 2020, AnGeo, 38, 789
Bordi, I., Berrilli, F., & Pietropaolo, E. 2015, AnGeo, 33, 267
Bushby, P., & Mason, J. 2004, A&G, 45, 4.7
Cameron, R. H., Jiang, J., & Schüssler, M. 2016, ApJL, 823, L22
Carrasco, V. M. S., & Vaquero, J. M. 2021, RNAAS, 5, 181
Charbonneau, P. 2020, LRSP, 17, 4
Chatzistergos, T., Ermolli, I., Krivova, N. A., & Solanki, S. K. 2019, A&A, 625, A69
Consolini, G., Tozzi, R., & de Michelis, P. 2009, A&A, 506, 1381
Fiandrini, E., Tomassetti, N., Bertucci, B., et al. 2021, PhRvD, 104, 023012
Foukal, P., & Lean, J. 1988, ApJ, 328, 347
Galuzzo, D., Cagnazzo, C., Berrilli, F., Fierli, F., & Giovannelli, L. 2021, ApJ, 909, 191
Gnevyshevl, M., & Ohl, A. 1948, AZh, 25, 18
Gupta, M., Mishra, V. K., & Mishra, A. P. 2007, JGRA, 112, A05105

Hathaway, D. 2015, LRSP, 12, 87
Hathaway, D., Hathaway, D., & Reichmann, J. 1994, SoPh, 151, 177
Hazra, G., Karak, B. B., Banerjee, D., & Choudhuri, A. R. 2015, SoPh, 290, 1851
Hudson, H. S. 1988, ARA&A, 26, 473
Janssens, J. 2021, JSWSC, 11, 3
Kopp, G., Krivova, N., Wu, C. J., & Lean, J. 2016, SoPh, 291, 2951
Labonville, F., Charbonneau, P., & Lemerle, A. 2019, SoPh, 294, 82
Lockwood, M., & Ball, W. T. 2020, RSPSA, 476, 2238
Mandal, S., Krivova, N. A., Solanki, S. K., Sinha, N., & Banerjee, D. 2020, A&A, 640, A78
Matthes, K., Funke, B., Andersson, M. E., et al. 2017, GMD, 10, 2247
McIntosh, S. W., Chapman, S., Leamon, R. J., Egeland, R., & Watkins, N. W. 2020, SoPh, 295, 163
Meadows, V. S., & Barnes, R. K. 2018, in Handbook of Exoplanets, ed. H. J. Deeg & J. A. Belmonte (Cham: Springer), 57
Mursula, K., Usoskin, I. G., & Kovaltsov, G. A. 2001, SoPh, 198, 51
Petrie, G., Criscuoli, S., & Bertello, L. 2021, Solar Magnetism and Radiation (Washington, DC: AGU), 83
Petrovay, K. 2020, LRSP, 17, 2
Plainaki, C., Antonucci, M., Bemporad, A., et al. 2020, JSWSC, 10, 6
Press, W. H., Teukolsky, S. A., Vetterling, W. T., & Flannery, B. P. 1992, Numerical Recipes in C (Cambridge: Cambridge Univ. Press)
Schwenn, R. 2006, LRSP, 3, 2
Singh, P., Saad Farid, A., Singh, A., Pant, T., & Aly, A. A. 2021, Ap&SS, 366, 48
Takalo, J. 2021, SoPh, 296, 80
Takalo, J., & Mursula, K. 2020, A&A, 636, A11
Tlatov, A. G. 2013, ApJL, 772, L30
Upton, L. A., & Hathaway, D. H. 2018, GeoRL, 45, 8091
Usoskin, I. G., Mursula, K., Solanki, S. K. M. S., & A., K. G. 2002, JGRA, 107, 1374
Vecchio, A., Lepreti, F., Laurenza, M., Alberti, T., & Carbone, V. 2017, A&A, 599, A58
Versteegh, G. 2005, SSRv, 120, 243
Volobuev, D. 2009, SoPh, 258, 319
Wilson, O. C. 1978, ApJ, 226, 379
Zolotova, N. V., & Ponyavin, D. I. 2015, Ge&Ae, 55, 902